

# CHAPTER IV

MORPHOLOGY & PROPERTIES OF  
BLENDS OF POLYHYDROXY-ALKANOATES  
AND LIGNIN DERIVATIVES.

## **CHAPTER IV**

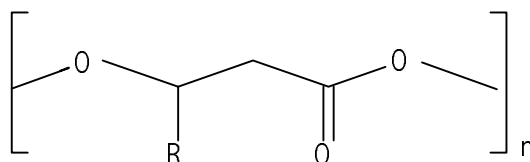
# **MORPHOLOGY & PROPERTIES OF BLENDS OF POLYHYDROXY-ALKANOATES AND LIGNIN DERIVATIVES.**

## **ABSTRACT**

Poly-3-hydroxybutyrate (PHB) and poly-3-hydroxybutyrate-co-3-hydroxyvalerate (PHBV) were blended in melt and solution with organosolv lignin (L) and organosolv lignin butyrate (LB). In the presence of lignin component, crystallization was inhibited or retarded for PHB blends revealing polymer-polymer interaction between PHB and lignin components. Shifting of glass transition temperatures was observed for PHB/L blends and the amount of crystallinity was lower for PHB/L as compared to PHB/LB blends, revealing greater interaction between PHB and L as opposed to LB. LB blends also revealed some interaction with PHBV and significantly reduced crystallinity in the samples. Melt processed samples of PHBV/LB had higher crystallinity compared to solvent cast blends possibly due to reduction in molecular weight owing to degradation. Mechanical properties reflected the morphological characteristics presented by the thermal measurements. All the blends had higher modulus than the native polymers (PHB and PHBV). Improvement in tensile strength and elongation at break was drastic in case of PHB/L blends.

## INTRODUCTION

Bacterially produced polyhydroxyalkanoates such as poly-3-hydroxybutyrate (PHB), are potentially very important biodegradable and biocompatible thermoplastic polymers [Doi (1990)]. PHB is highly crystalline and very brittle which reduces its possible use as a useful thermoplastic polymer. Copolymerization with hydroxyvalerate by feeding the bacteria with propionic acid, provides a solution to the above problem [Holmes (1988)]. The structure of a typical polyhydroxyalkanoate repeat unit is



### Poly-3-hydroxyalkanoate

where, R represents  $\text{CH}_3$  for beta-hydroxybutyrate, or  $\text{C}_2\text{H}_5$  for beta-hydroxyvalerate.

Random copolymers can crystallize between two well defined extremes: (1) complete exclusion of the non-crystallizable comonomer [Flory (1955)], and (2) uniform inclusion of co-units [Sanchez and Eby (1975)]. In case of PHBV, the first extreme case is not possible since both the co-monomer units readily co-crystallize [Orts et.al. (1991)]. Crystallization studies on PHBV copolymers showed similar results as that of homopolymer PHB, though the rates of growth and nucleation are significantly lower in the copolymers due to considerable exclusion of hydroxyvalerate (HV) from the crystals, specially at higher HV content and at high crystallization temperatures [Organ and Barham (1991)].

Due to high cost of producing these polymers, polyhydroxyalkanoates are presently used only for special medical applications [Holmes (1988)]. However, in order to use these polymers as commodity plastics, the price has to be sufficiently lowered without affecting the useful properties of the original polymer. Blending with other biopolymers provides a solution to this problem. Studies on blends of poly-3-hydroxybutyrate-co-3-hydroxyvalerate (PHBV) with cellulose esters such as cellulose acetate butyrate and cellulose acetate propionate revealed single glass transitions up to 50% concentration of PHBV and followed the Fox equation for miscible systems [Lotti and Scandola (1992)]. For concentrations of PHBV higher than 50%, crystallization of PHBV separated the two polymer phases and separate transitions were observed. Similar results were presented for the blends of the homopolymer PHB by the authors earlier. Incorporating maize starch granules into PHB and PHBV revealed that destructured starch produces a greater reinforcing effect than native starch granules with increase in modulus [Koller and Owen (1996)]. Also crystallinity in PHBV was increased with incorporation of starch without affecting nucleation.

The present study is based on modifying the properties of PHB and PHBV by blending with lignin and lignin derivatives. Lignin is a small molecule and acts as a reinforcement for many other polymers such as poly(methyl methacrylate) [Ciemniecki and Glasser (1988)]. Moreover, it is biodegradable and so can suitably be blended with PHB and PHBV without losing their biodegradable properties. Lignin has been found to act as a nucleating agent for other crystalline polymer systems [Willer and Glasser

(1994)]. Moreover, recent unpublished studies have shown the possible use of lignin as a plasticizer/antiplasticizer as well as a rheology modifier. This study would discuss some of the roles played by the lignin in blends with PHB and PHBV.

## EXPERIMENTAL

### MATERIALS

Poly(hydroxybutyrate) (PHB) and poly (hydroxybutyrate-co-hydroxyvalerate) (PHBV) were obtained as white powder (technical grade) from Biopol (Marlborough Biopolymers), Cleveland, UK. PHB is a pure homopolymer whereas PHBV is a copolymer of hydroxybutyrate and hydroxyvalerate. The average hydroxyvalerate content in PHBV was 15.6% (Product ref. MBL 100/1298).

Organosolv Lignin (L) was obtained from Aldrich Chemical Company, WI, USA (Catalog #: 37,101-7). The glass transition and thermal decomposition temperatures are 107°C and 308°C, respectively. The average molecular weight  $M_w$  and  $M_n$  are 3,140 and 820 respectively with a MWD of 3.8.

Organosolv Lignin Butyrate (LB) was prepared by esterification of organosolv lignin as mentioned in chapter II of this thesis. The glass transition temperature of lignin butyrate and thermal decomposition temperatures are 54°C and 308°C respectively. The average degree of substitution of butyrl group was 0.69. LB was obtained as a brownish-black powder. The powders were dried under vacuum at 35 °C for 12 hours before being blended.

### METHODS

#### Blend Preparation

PHB/L and PHB/LB blends of 100/0, 90/10, 80/30 and 70/30 were prepared by melt processing. PHBV/LB blends of 100/0, 90/10, 80/20, 70/30, and 50/50 by weight were prepared by solvent casting and melt extrusion. For preparation of the blends by solvent casting with LB, the blend components were stirred in chloroform (blend concentration of approximately 5% by weight of the solution) at room temperature until all the material was totally dissolved. The solution was then cast in teflon molds and kept at room temperature in a dessicator for 72 hours so as to evaporate the solvent (chloroform) in a controlled manner. The solvent cast blend was then put in a vacuum oven at 35 °C for 12 hours to remove any remaining solvent.

For preparation of blends by melt extrusion, corresponding amounts of individual components were physically mixed at room temperature in a beaker until the color of the mixture looked homogeneous. The mixed powder was then transferred to a preheated "Mini-Max" injection molder from Custom Scientific Instruments. It was observed that after the addition of even a small amount of L or LB, the blends could be processed at a lower temperature than that for native PHB or PHBV. Therefore, to avoid any degradation of PHB or PHBV, the processing temperature was maintained at 190°C for native polymer and lowered to 160-140°C for higher L or LB containing blends. The powder was placed inside the barrel of the molder where it was melted and blended. The polymer was blended in the melt for approximately one minute before it was injected into

the mold. The mold cavity was heated through conduction from the fixture and the polymer melt during the injection process and so can be considered as a preheated mold. The cooling rate was not controlled after injection. Consequently, the specimens should be considered to have been quenched.

Two types of specimens were molded: rectangular DMTA specimens and dog bone Minimat specimens. Rectangular specimens had dimensions of 38 mm x 12.6 mm x 1.6 mm. Dog bone specimens, had a nominal length of 38 mm long with a gage section measuring 10 mm x 2.7 mm x 3.0 mm.

### **Differential Scanning Calorimetry (DSC)**

The thermal analysis of the samples was determined on a Perkin-Elmer Model DSC-4 equipped with a Thermal Analysis Data Station (TADS) using standard aluminum pans. The temperature was scanned from  $-40$  to  $180^{\circ}\text{C}$  at scanning rates of  $2.5$  and  $10^{\circ}\text{C}/\text{min}$ . Nitrogen was used as a sweeping gas. The instrument was calibrated with an indium standard. The glass transition temperature and the heat of fusion were reported from the second heating scan, unless otherwise indicated. The glass transition temperature ( $T_g$ ) was taken as the temperature at the midpoint ( $1/2 \Delta C_p$ ) of the transition. The melting temperature ( $T_m$ ) is reported as the peak value of the melting endotherms. The crystallization temperatures were reported from the first cooling scans from melt.

### **Dynamic Mechanical Thermal Analysis (DMTA)**

The dynamic mechanical properties of the blend samples were determined in a dynamic mechanical thermal analyzer (DMTA) by Polymer Laboratories Ltd.; Shropshire, England. The samples were loaded horizontally in DMTA standard medium size clamps. Measurements were performed in the single cantilever bending mode. The spectra were collected from  $-20^{\circ}\text{C}$  to  $150^{\circ}\text{C}$  at a heating rate of  $4^{\circ}\text{C}/\text{min}$  at a frequency of  $1.0$  Hz. The final temperature of scan varied from sample to sample depending on the onset of melting where the value of  $\tan \delta$  was above limits and the DMTA was out of balance.

### **Mechanical Properties**

The mechanical properties (modulus, strength and ultimate strain) of the blends were determined on a Miniature Materials Tester (Minimat model # SM9-06) by Polymer Laboratories Ltd., Loughborough, England. Tests were conducted at room temperature with a  $1000$  N load cell using a strain rate of  $0.25$  mm/min. The calculation of modulus and strength was based on the initial cross sectional area. The data reported represent the average of five measurements for each blend composition.

### **Transmission Electron Microscopy (TEM)**

Samples of 20%LB/PHBV were embedded in Poly/Bed 812 (Polysciences, Inc.) cured at  $60^{\circ}\text{C}$  for 48 hours in flat molds.  $80$ - $100$  nm thick sections were cut from the embedded films with a diamond knife mounted on a Reichert Ultracut E microtome. The sections were carefully mounted on copper grids. The grids were observed on a JEOL JEM-100CX-II electron microscope operated at an accelerating voltage of  $80$  kV. The

micrographs were from the bright field images of the cut unstained samples at magnifications of 4,800x and 10,000x.

## RESULTS AND DISCUSSION

### PHB BLENDS

#### • DSC Results

DSC scans of the native PHB showed a sharp exothermic peak at 81.5<sup>0</sup>C and an endotherm at 173<sup>0</sup>C corresponding to the crystallization and melting respectively of the homopolymer (Fig. 4.1 and Table 4.1). The value of the melting peak of 173<sup>0</sup>C is lower than the published value of 195 ± 5 <sup>0</sup>C [Barham et.al. (1984)] probably due to differences in the molecular weights as well as the heating rate resulting in shorter crystallization times. However, the DSC scans of melt processed PHB revealed a broader crystallization peak occurring at 78<sup>0</sup>C (lower than that for native PHB) (Fig.4.1). This is possibly due to the reduction in the molecular weight owing to degradation of PHB while melt processing as also reported by Edie and Marand [Edie and Marand (1991)]. But melt processed PHB has  $\Delta H_c$  or  $\Delta H_m$  values greater than native PHB (Table 4.1). This might be due to the dependence of crystallization kinetics with molecular weight. However, when the melt processed PHB is scanned at a slower rate (2.5<sup>0</sup>C), crystallization occurs at a higher temperature (105<sup>0</sup>C) as expected, due to longer crystallization times (Fig.4.1). When the PHB sample was quenched from melt, a sharp second order transition related to the glass transition of PHB was observed at around 0<sup>0</sup>C in the subsequent heating scan.

When L or LB was added to PHB, crystallization was retarded due to the presence of the lignin component. The DSC curves for PHB/L blends are shown in Fig.4.2. At a cooling rate of 10<sup>0</sup>C/min, no crystallization was observed for any of the PHB/L blends. Cooling at a slower rate (2.5<sup>0</sup>C/min) revealed some crystallization of 10%L/PHB blend due to longer crystallization times. However, addition of 20% L to PHB further retarded crystallization at a cooling rate of 2.5<sup>0</sup>C/min (Fig.4.2). Therefore, the crystallinity in PHB is lower when higher amount of L is present possibly due to the dilution effect. This reveals interaction between PHB and L or LB (data not shown). This is a good sign from the fact that most of the undesirable properties of PHB such as brittleness results from the high crystallinity and cracks formed in spherulites [Barham and Keller (1986)].

However, cold crystallization was observed for all the blends during the subsequent heating cycle at a scanning rate of 10<sup>0</sup>C/min followed by melting (Fig.4.2). DSC curves from the second heating scans for blends of PHB and L revealed cold crystallization and melting (Fig. 4.3). The first curve with no lignin in Fig.4.3 represents the heating scan of PHB quenched from melt in order to observe the  $T_g$  of PHB. Glass transitions are very prominent in case of all blend compositions. The glass transitions of the blends show an increasing trend and the values are about 7 to 11<sup>0</sup>C higher than pure PHB (Table 4.1). This reflects the effect of molecular interaction between PHB and L on the  $T_g$  of PHB. The glass transition of L was reported earlier (in chapter II) as 107<sup>0</sup>C.  $T_g$ 's corresponding to the L component is not pronounced compared to those from the PHB phase, however, faint transitions are observed near 100<sup>0</sup>C for the blends corresponding to L component. The  $T_m$ 's do not vary significantly with the L content in blend, though cold

crystallization temperatures increase (Table 4.1). Therefore, it can be understood that there exists some polymer-polymer interaction between L and PHB. Also, lignin acts as an anti-plasticizer for PHB.

In case of PHB/LB blends, the glass transition of LB has been eclipsed by the exothermic crystallization peak of PHB in the temperature range of 45 to 90°C in all cases. Annealing the samples by very slow cooling was attempted in order to observe the glass transition of LB by minimizing the exothermic crystallization peak. In all the cases of slow cooling, some amount of cold crystallization was observed in the consecutive heating scans and the glass transition corresponding to LB was not observed (Fig.4.4). In all the cases, sharp second order transitions near the glass transition of PHB were observed. The  $T_c$  values for PHB/LB blends shift towards higher temperatures and the crystallization peaks become broader with increasing amount of LB (Fig.4.4). No specific conclusions can be made at this stage without further investigations of the crystal lattice structure, dimensions and crystallization kinetics. Also there is not much or no elevation in the  $T_g$  values for PHB/LB as compared to PHB/L blends (Fig.4.5). Moreover, the normalized  $\Delta H_m$  values for PHB/LB are higher than those for PHB/L blends (Fig.4.6). This might be an indication of greater interaction between PHB and L as compared to PHB and LB. On the other hand, the  $T_m$  values for PHB/LB blends are observed to shift towards lower temperatures (Table 4.1). This reveals that the crystallization process is retarded. Also, an emergence of a side peak is observed and this peak becomes prominent at higher LB concentrations (Fig.4.4). This might be attributed to the lamellar thickening that occurs while crystallization. The normalized  $\Delta H_m$  values for the blend compositions of up to 20% LB are equal to that of pure PHB. This reveals that the PHB component in the crystalline phase of the blend can retain its original degree of crystallinity even when LB is added. At 30% LB concentration, possibly the amount of LB is high enough to hinder the growth of crystals due to dilution effect and therefore, the value of  $\Delta H_m$  decreases.

#### • DMTA Results

Dynamic mechanical thermal analysis results reveal clear indications of the shifts in the glass transitions of PHB towards higher temperatures when L or LB is present (Fig. 4.7 and 4.8). In both the blends of PHB with L and LB, the  $\tan \delta$  curves as well as  $E''$  curves representing the glass transition behavior of PHB component in blend shift towards higher temperatures whereas no clear separate peaks showing the glass transitions of L and LB are observed. This might be due to the fact that the lignin components are entrapped within the spherulitic structures of PHB and so the glass transitions arising from the lignin component are suppressed. The transitions associated with L and LB might have been prominent if the L and LB had been present in much greater concentrations. This predicts interaction between PHB and L or LB revealing some interaction between the two components.

#### • Mechanical Properties

When the polymer pairs exist in two phases, the mechanical properties of the blend material are governed by the distribution of the properties of the respective polymers within the blend. In other words, the properties are related to mainly the higher volume polymer phase, which usually forms the continuous matrix, while the secondary phase plays the role of reinforcing the matrix by adequate stress transfer between interphases. Lignin is a small molecule and acts as reinforcing filler when it is in glassy state, i.e. below its  $T_g$ . This effect has been detected earlier in case of blends of hydroxypropyl lignin and poly(methyl methacrylate) [Ciemniecki and Glasser (1988)]. The mechanical properties indicate improvement in tensile strength, strain at break and modulus when LB or L are incorporated (Fig.4.9). The increase in modulus is expected because LB and L both act as reinforcing filler as explained earlier (Fig.4.9c). But modulus decrease is also expected since the amount of crystallinity decreases in PHB. These are two competing effects and from the results it is found that the effect of crystallinity is less pronounced than the reinforcing effect of L and LB. Also the molecular weight of L being much lower than LB, probably the sizes of the L molecules are smaller than those for LB. Therefore, the reinforcing effect of smaller particles is expected to be higher than that of larger particles. This is valid since the modulus increase in case of L is much greater than that for LB.

The tensile strength depends largely on the ease of stress transfer between the phases present in the blend, greater stress transfer leading to higher strength. In all blends of lignin with other polymers such as poly(methyl methacrylate), modulus increase has been observed with decrease in tensile strength [Ciemniecki and Glasser (1988)]. Since lignin is a glassy material, it is not expected to increase tensile strength of the blends. But in case of blends with PHB, an increase in tensile strength is also observed. This might be attributed to the decrease in the crystallinity in PHB with incorporation of L or LB. More of PHB is present as amorphous material than that in crystalline phase in the blends and so adequate stress transfer is more probable between two amorphous phases than between crystalline and amorphous phases. Also this might be a possible explanation since the amount of increase in tensile strength of L blends is much more than that of LB blends (Fig.4.9a), since the amount of crystallinity in PHB/L blends is lower compared to PHB/LB blends at similar blend compositions (Table 4.1). Another reason of higher strength in case of L blends might be due to better interaction between PHB and L as evidenced from the DSC results already discussed earlier and therefore, better stress transfer between phases is possible. The PHB/LB blend samples were more brittle as compared to PHB/L blends and powdered material was obtained when a PHB/LB sample was cut with a sharp edge. Whereas, chunks of thin slices were obtained when a PHB/L blend material was cut.

PHB is usually quite brittle and low strains at break are observed in PHB mainly due to cracks in the spherulites [Barham and Keller (1986)]. These cracks may be either radial or circumferential depending on the crystallization temperatures and are formed under no externally applied stress. When the material is strained, the cracks propagate and join together leading to a brittle failure. So brittleness can be decreased either by healing of the cracks (usually by cold rolling process) or by decreasing the amount of crystallinity. In the latter case, the amorphous portion can elongate to certain extent more compared to crystalline regions and distribute the stress without concentrating at a particular area. This diminishes the propagation of cracks. Therefore, the elongation at



break also increases to certain extent if crystallinity is reduced. This is observed in the PHB blends where the ultimate strain increases by 50% in case of 10% of L or LB content (Fig. 4.9). At this composition, the overall crystallinity is found to decrease by more than 15% (Table 4.1). Also decrease in normalized  $\Delta H_m$  in case of L blends is more than that for LB blends (Fig. 4.6) and so correspondingly, increase in strain for L blends is greater than LB blends. This can also be attributed to higher polymer-polymer interaction between L and PHB as explained earlier. At higher L or LB contents, the blend becomes more brittle due to higher glassy lignin content and so the ultimate strain value declines at higher L or LB contents.

## PHBV BLENDS

### • DSC Results

DSC scans of native PHBV reveal a sharp glass transition at  $-2^{\circ}\text{C}$  and two endothermic peaks at around 145 and  $160^{\circ}\text{C}$  (Fig. 4.10 and Table 4.2) which is consistent with the earlier published result [Organ and Barham (1991)]. The presence of two melting peaks is attributed to the lamellar thickening, which occurs even for high heating scan rates. Also the ratio of the original (lower) melting peak to the higher melting peak depends on various factors such as crystallization temperature as well as the hydroxyvalerate (HV) content in the copolymer. It has been found that for lower crystallization temperatures, greater thickening occurred and the original peak was barely recognized. For higher HV content copolymers, the crystallization kinetics is much more complex and five melting peaks were reported [Organ and Barham (1991)]. Crystallization was observed during the cooling scan when the sample was cooled from melt at a slow rate of  $10^{\circ}\text{C}/\text{min}$  (Not shown). Native PHBV crystallized while cooling only for low cooling rates. But hardly any crystallization occurred when the sample was quenched from melt revealing slower crystallization kinetics for PHBV. In case of quenched samples, cold crystallization occurred when it was subsequently heated at a rate of  $10^{\circ}\text{C}/\text{min}$ . The heat of crystalline melting ( $\Delta H_f$ ) values for PHBV is lower (36 J/gm) as compared to 83 J/gm in case of PHB (Table 4.1 and 4.2). The lower crystallinity in PHBV makes it more useful than PHB for applications.

DSC scans of blends of PHBV and LB prepared by solvent casting as well as melt blending show decreasing trends in crystallinity as the LB content increases (Figs 4.10, 4.11 and 4.12). For solvent cast samples, at 30% LB content, crystallinity is quite pronounced when the samples are quenched from melt but hardly any crystallinity is observed if it is cooled slowly (compare Figs. 4.10 and 4.11). This might be attributed to spontaneous orientation of the chains of PHBV occurring at a temperature higher than the glass transition temperature of the copolymer when heated rather than orientation taking place in molten state while cooling. At higher LB content (50%) no crystallinity is observed in either cases of solvent cast blends (Figs. 4.10 and 4.11), though some crystallinity is evident from the blends prepared by melt blending (compare curves at 50% LB in Figs. 4.11 and 4.12). Therefore, similar to the results discussed for PHB blends, there exists some interaction between LB and PHBV and hence LB retards the crystallization of PHBV. In case of melt processed samples, PHBV is degraded to some extent and weight average molecular weight ( $M_w$ ) decreases. Similar to other semi-

crystalline polymers, the crystallization process is dependent on the molecular weight of PHBV and the rate of crystallization peaks at a certain  $M_w$  and again decreases for higher  $M_w$ . Therefore, the rate of crystallization is enhanced at a lower  $M_w$  for melt processed PHBV and crystallinity is greater in melt processed than solvent cast PHBV blends.

- **DMTA Results**

Both the  $\tan \delta$  and  $E''$  curves show a broadened peak near  $10^\circ\text{C}$  which conforms with the relaxations associated with the glass transition phenomenon of PHBV (Fig.4.13). Also the peaks shift towards higher temperatures indicating some interaction between the PHBV and LB. The  $\tan \delta$  peaks are also elevated after the glass transition of PHBV as the LB content increases. This reveals the emergence of the relaxations associated with the glass transitions of LB around  $50^\circ\text{C}$ . This transition might become more prominent if the LB content is sufficiently higher. This might also indicate that the average dimensions of LB phase increases with increase in LB content in the blend. Since the blends are crystalline (except that of 50% LB content), no sharp decline in the storage modulus curves are observed near the  $T_g$ 's of the components. The decline starts at the onset of melting of the crystals at temperatures above  $100^\circ\text{C}$  (not shown here) though gradual decline is observed over the entire temperature range. But for 50% LB content, the decline starts after the  $T_g$  of LB since the amount of crystallinity is very less. Therefore, LB can retain the modulus of the blends till the  $T_g$  of LB is reached though PHBV is in rubbery state.

- **TEM Results**

Transmission electron micrographs reveal distinct phases for PHBV and LB (Fig.4.14). LB phase can be distinguished from the PHBV phase by the dark color of LB phase. However, it is noted from the wavy pattern of the bright regions that the PHBV phase contains some amount of LB. This reveals some interaction between PHBV and LB and possibly some amount of LB goes into the PHBV phase whereas the rest of LB is segregated into distinct LB phase. This is consistent with the thermal results. It was not possible to magnify the PHBV phase any further above 10,000x because the microtomed specimen began to tear apart as the electron beam was concentrated at a smaller area.

- **Mechanical Properties :**

PHBV is a copolymer and possesses lower crystallinity than PHB. So being in the rubbery state at ambient temperatures, PHBV shows higher strain and tensile strength than PHB. With the incorporation of LB into PHBV phase, stress transfer in the continuous PHBV phase is hindered due to the presence of glassy LB phase. Therefore, a decline in tensile strength is observed with increasing LB content (Fig.4.15). The ultimate strain decreases rapidly when the LB content is more than 20%. This effect is not due to the amount of crystallinity present in the blend since lower crystallinity should show better stress transfer in the amorphous phases. It is due to the higher amount of glassy material (LB) present in the blend and this makes it more brittle. This is particularly true since an increase in modulus is observed around 20% LB content.

## CONCLUSIONS

DSC and DMTA results revealed interaction between the PHB and L or LB. Crystallization was retarded by the presence of lignin component revealing interaction between PHB and lignin components. The glass transitions of PHB in the blends were shifted towards higher temperatures, though enough evidence was found of another relaxation present near the glass transitions of L or LB. Higher amounts of crystallinity were observed in case of PHB/LB as compared to those of PHB/L blends at the same composition ratios. This gives an idea that the interaction between L and PHB is more pronounced than LB. This is very important from the point of view of application since brittleness can be reduced in PHB. Similar decrease in crystallinity was observed for PHBV blends. Crystallinity in PHBV decreases to almost zero when 30% LB is present. Crystallinity observed in case of solvent cast films is less than that for melt blended samples due to higher  $M_w$ . Modulus increase in blends of PHB and PHBV with L and LB has been accounted for the reinforcing property of glassy lignin molecules. But increase in tensile strength and ultimate strain is observed in both PHB/L and PHB/LB blends. L or LB significantly enhances the mechanical properties in PHB when blended and can be used to modify PHB for useful applications. Significant increase in modulus is also useful for specific applications of PHB and PHBV.

## FUTURE WORK

Recommendations for future work include :

- 1) The present study covered in this chapter is not sufficient to reveal any form of miscibility of the blend components. So further crystallinity studies are necessary to test whether the blends of PHB or PHBV with L or LB are miscible. The blend miscibility characteristics can be performed by using the well established Flory-Huggins relationship using the equilibrium melting temperatures from the Hoffman-Weeks plots.
- 2) Rheological studies of the blends can be carried out in order to understand the effect of the lignin component on the melt viscosity and processing conditions of the blends.
- 3) The effect of the lignin component on the molecular weight of PHB or PHBV when processed at a temperature range above 150°C should be studied. This would suggest the degradation characteristics of the polyhydroxyalkanoates in the presence of lignin component. Lignin is observed to be an electron absorbing species and can reduce the chances of oxidation (hence degradation) of the polyhydroxyalkanoates.

## REFERENCES

- Barham, P. J. and Keller, A. (1986), The relationship between Microstructure and mode of Fracture in Polyhydroxybutyrate, *Journal of Polymer Science: Polymer Physics Edition*, Vol. 24, 69-77.
- Barham, P. J., Keller, A., Otun, E. L. and Holmes, P. A. (1984), Crystallization and morphology of a bacterial thermoplastic: poly-3-hydroxybutyrate, *Journal of Materials Science*, 19, 2781-2794.
- Ciemniecki, S. L. and Glasser, W. G. (1988), Multiphase materials with lignin: 1. Blends of hydroxypropyl lignin with poly(methyl methacrylate), *Polymer*, Vol. 29, 1021-1029.
- Doi, Y. (1990), “*Microbial Polyesters*”, VCH Publishers, New York.
- Edie, S. L., and Marand, H. (1991), “Study of Miscible Blends of Poly(vinylidene fluoride) and Poly(3-hydroxybutyrate)”, A.C.S. Polym. Preprints, 32(2), 329-330.
- Flory, P. J.(1955), *Trans. Faraday Soc.*, 51, 848.
- Holmes, P. A.,(1988), Biologically produced (R)-3-hydroxy-alkanoate polymers and copolymers. In: Basset, D.C. (ed.) “*Developments in Crystalline Polymers*”, Elsevier, New York, Vol.2, pp.1-65.
- Koller, I; and Owen, A. J. (1996), Starch-Filled PHB and PHB/HV Copolymer, *Polymer International*, 39, 175-181.
- Lotti, N and Scandola, M (1992), Miscibility of bacterial poly(3-hydroxybutyrate-co-3-hydroxyvalerate) with ester substituted celluloses, *Polymer Bulletin* 29, 407-413.
- Organ, S. J. and Barham, P. J. (1991), Nucleation, growth and Morphology of poly (hydroxybutyrate) and its copolymers, *Journal of Material Science*, 26, 1368-1374.
- Orts, W. J, Bluhm, T. L. and Marchessault, R. H. (1991), *Macromolecules*, 24, 6435.
- Orts, W. J, and Bluhm, T. L. (1992), Melting Point Depression for Poly( $\beta$ -hydroxybutyrate-co- $\beta$ -hydroxyvalerate) Random Copolymers, *Polymer Preprints (ACS, Poly Chem)*, Vol 33, No 2, 530-531.
- Sanchez, I. C. and Eby, R. K. (1975), *Macromolecules*, 8, 638.
- Oliveira, Willer de, and Glasser, W.G., (1994) Multiphase materials with Lignin II .Starlike Copolymers with Caprolactone, *Macromolecules*, 27, 5-11.
- Yoshie, N.; Azuma, Y.; Sakurai, M.; and Inoue, Y. (1995), Crystallization and compatibility of Poly(vinyl alcohol)/Poly(3-hydroxybutyrate) Blends: Influence of Blend Composition and Tacticity of Poly(vinyl alcohol), *Journal of Applied Polymer Science*, Vol. 56, 17-24.

**Table 4.1 :** Thermal characteristics of blends of PHB.

	$T_g$ ( $^{\circ}\text{C}$ )	$T_m$ ( $^{\circ}\text{C}$ )	$T_c^*$ ( $^{\circ}\text{C}$ )	$\Delta H_c^*$ J/gm	$\Delta H_m$ J/gm	Normalized	
						$\Delta H_c$ J/gm of PHB	$\Delta H_m$ J/gm of PHB
PHB (native)	0.5	173.1	81.5	-61.3	87.6	-61.3	87.6
PHB (melt processed)	-	177.8	78.1	-63.3	92.8	-63.3	92.8
PHB/L Blends							
90/10	7.6	177	69*	-70.3*	71.1	-78.1	79.0
80/20	10.0	175	74*	-62.7*	64.2	-78.4	80.3
70/30	11.6	175	81*	-51.6*	53.1	-73.7	75.9
PHB/LB Blends							
90/10	4.3	170	63*	-73.7*	75.4	-81.9	83.8
80/20	2.4	161	75*	-64.6*	66.7	-80.8	83.4
70/30	1.8	156	80*	-50.8*	52.7	-72.6	75.3

\* The reported crystallization temperatures ( $T_c$ ) and heat of crystallization ( $\Delta H_c$ ) values for the blends are the peak temperatures of the crystallization endotherms observed in the second heating scans (usually reported as cold crystallization) at a scanning rate of  $10^{\circ}\text{C}/\text{min}$ . No crystallization was observed during the cooling scans at a scanning rate of  $10^{\circ}\text{C}/\text{min}$  for any of the blend samples. The  $T_c$  reported for PHB (without lignin component) are from the crystallization endotherms observed during the first cooling scans from melt at a cooling rate of  $10^{\circ}\text{C}/\text{min}$ .

**Table 4.2 :** Thermal characteristics of blends of PHBV and LB.

PHBV / LB Blends	$T_g$ ( $^{\circ}\text{C}$ )	* $T_m$ ( $^{\circ}\text{C}$ )		$\Delta H_m$ J/gm	Normalized $\Delta H_m$ J/gm of PHBV
Solvent ( $\text{CHCl}_3$ ) Cast					
100/0	-2.3	145	159	35.9	35.9
90/10	-1.5	138	154	29.3	32.6
70/30	2.1	--	155	1.12	1.6
50/50	-8.5	--	--	--	--
Melt Blended					
100/0	-2.1	142	159	37.4	37.4
90/10	0.1	145	159	30.7	34.1
80/20	2.5	140	155	30.2	37.8
70/30	-0.1	137	--	11.6	16.6
50/50	5.6	--	148	4.1	8.2

\* The two melting points correspond to the temperatures of the two melting endotherm peaks found for PHBV. Dashes show the absence of one or both peaks.

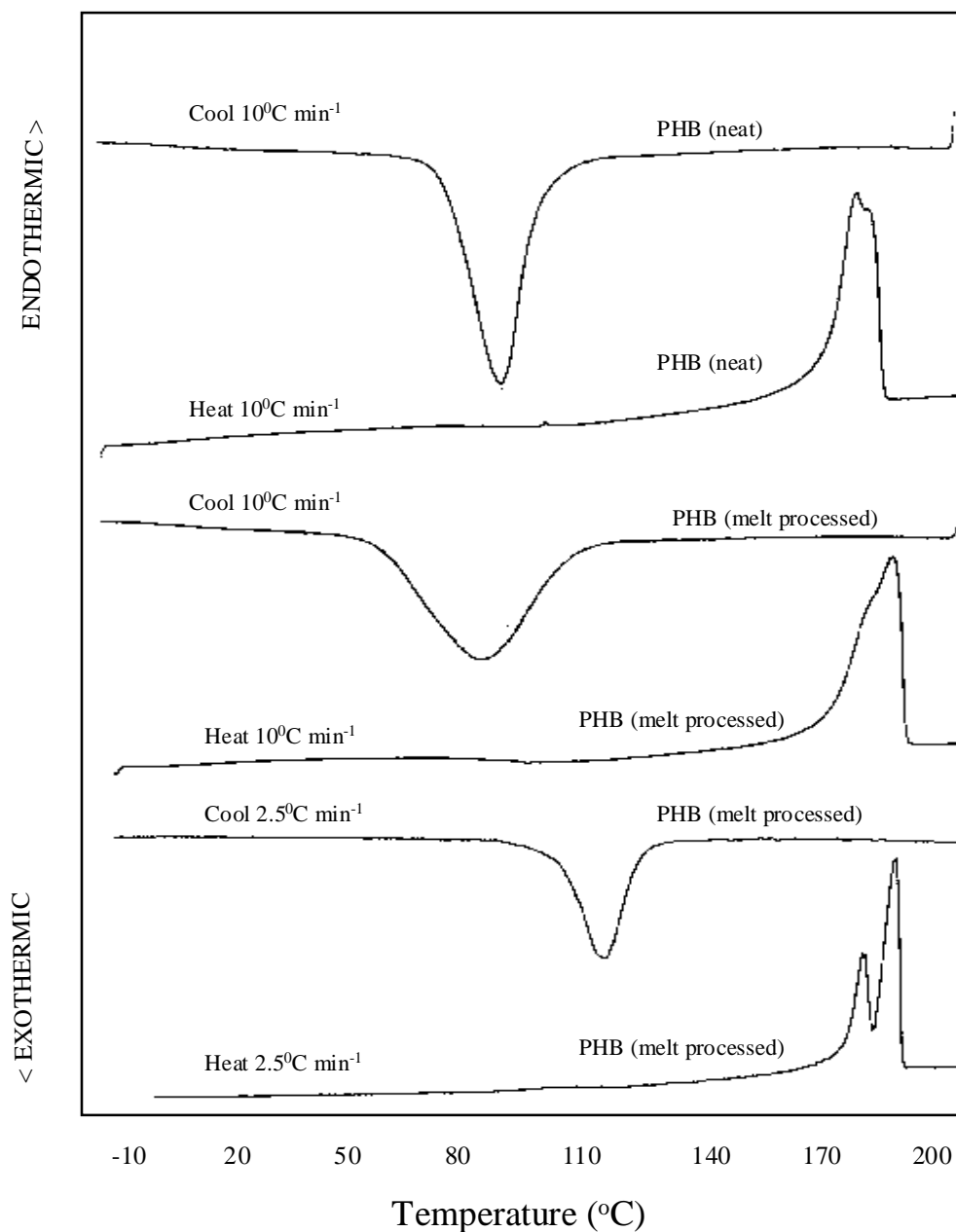


**Figure 4.1** : Effect of processing and crystallization times on PHB. The cooling traces are from the first cooling scans from melt and the heating traces are from the second heating scan. (Some curves have been expanded on the y-scale for greater clarity and so the y-axis has no significance).

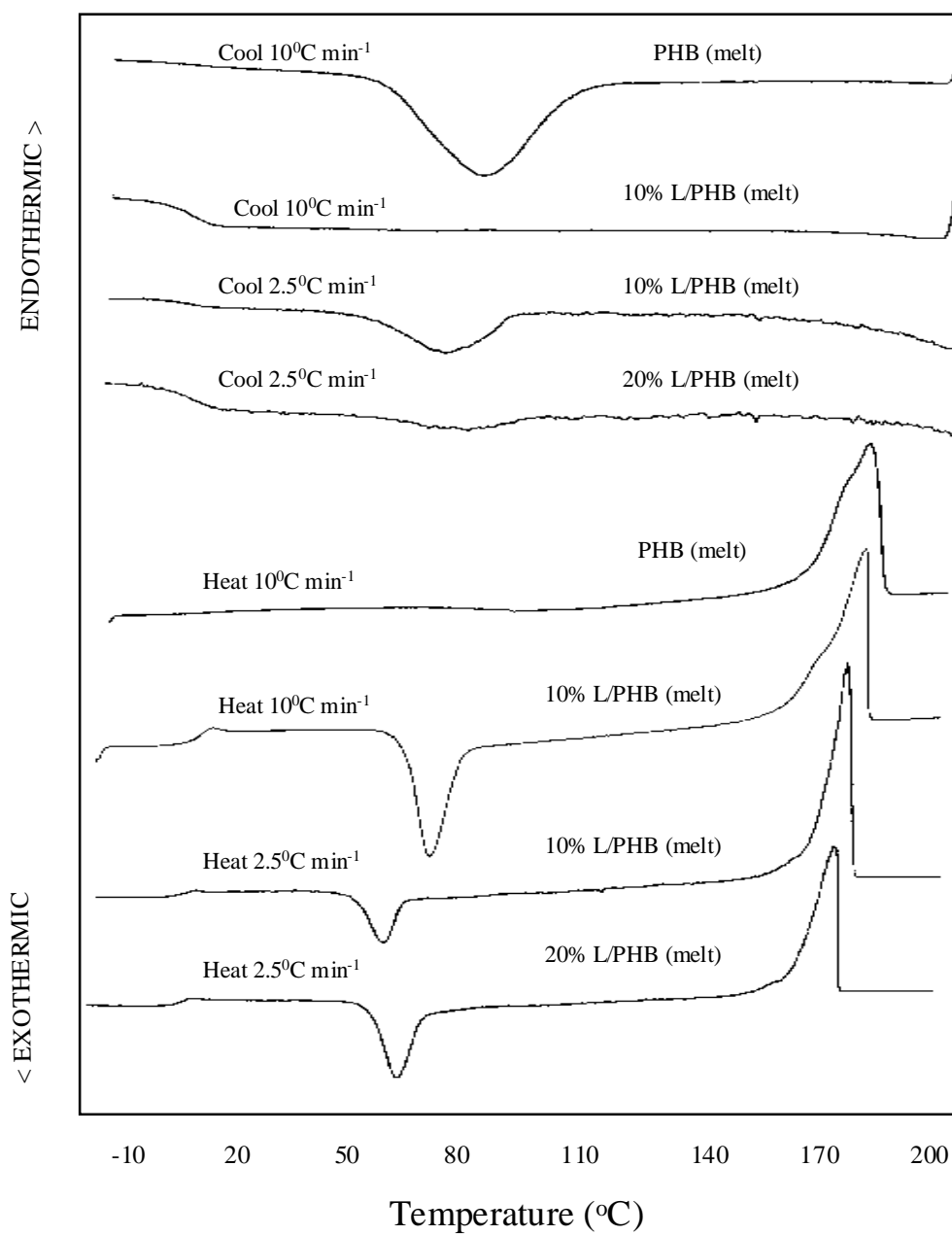


**Figure 4.2** : DSC thermograms of melt blended samples of PHB and L.



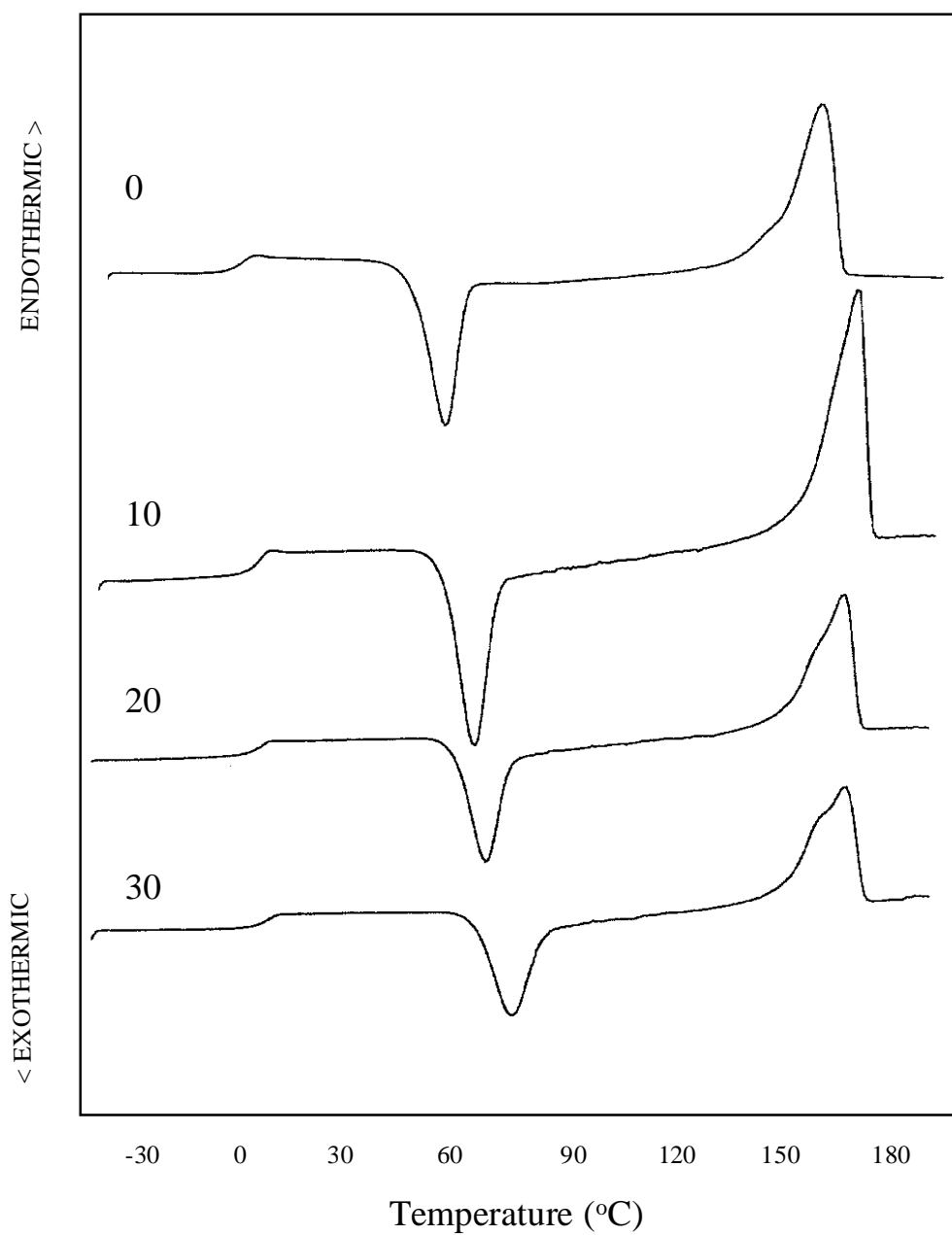


**Figure 4.3 :** DSC thermograms of melt blended samples of PHB and L. Numbers on each curve denote L content (wt.%) in the blend. These traces are from the second heating scan (after quenching from melt at a rate of 300 °C/min).

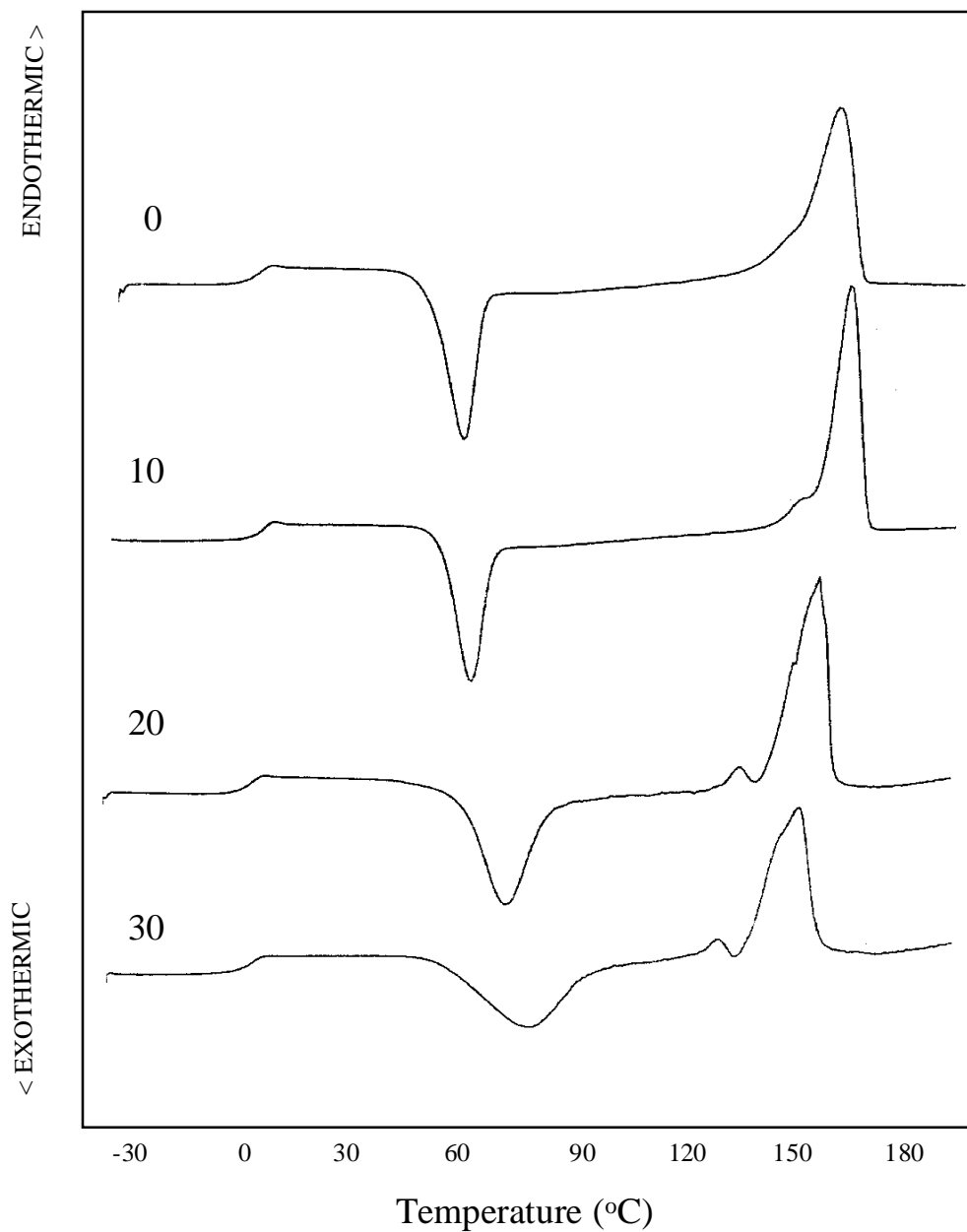


**Figure 4.4** : DSC thermograms of melt blended samples of PHB and LB. Numbers on each curve denote LB content (wt.%) in the blend. These traces are from the second heating scan (after quenching from melt at a rate of 300°C/min).

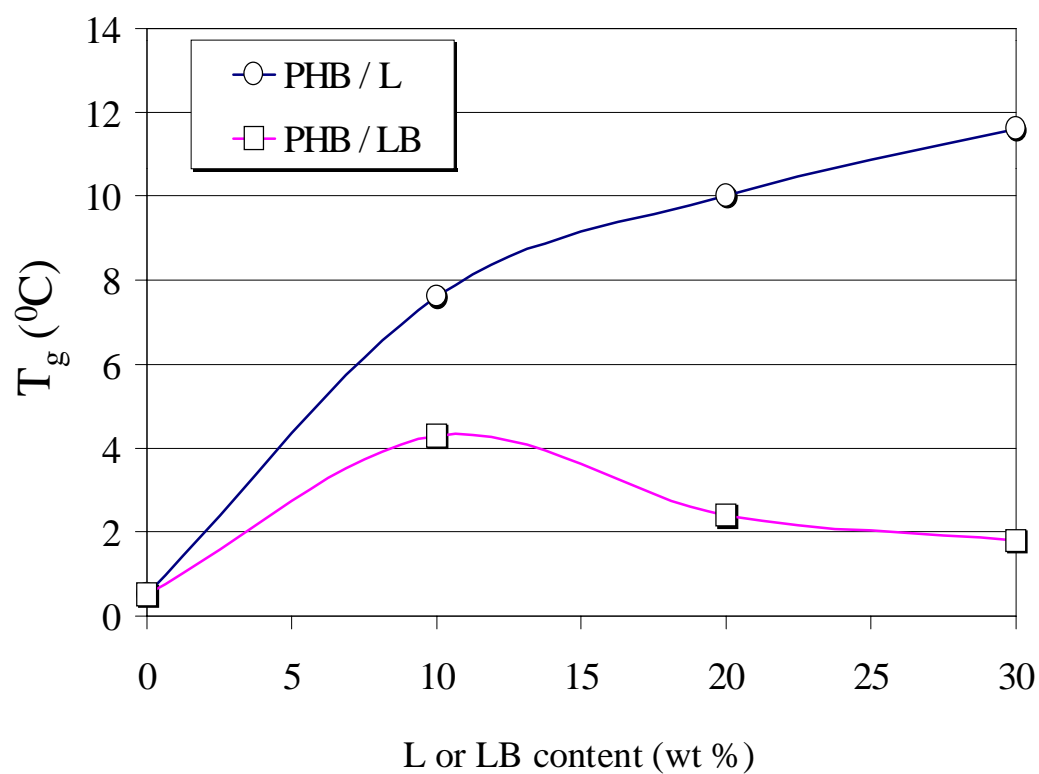


**Figure 4.5:** Glass transition temperatures ( $T_g$ ) for PHB and L or LB blends.

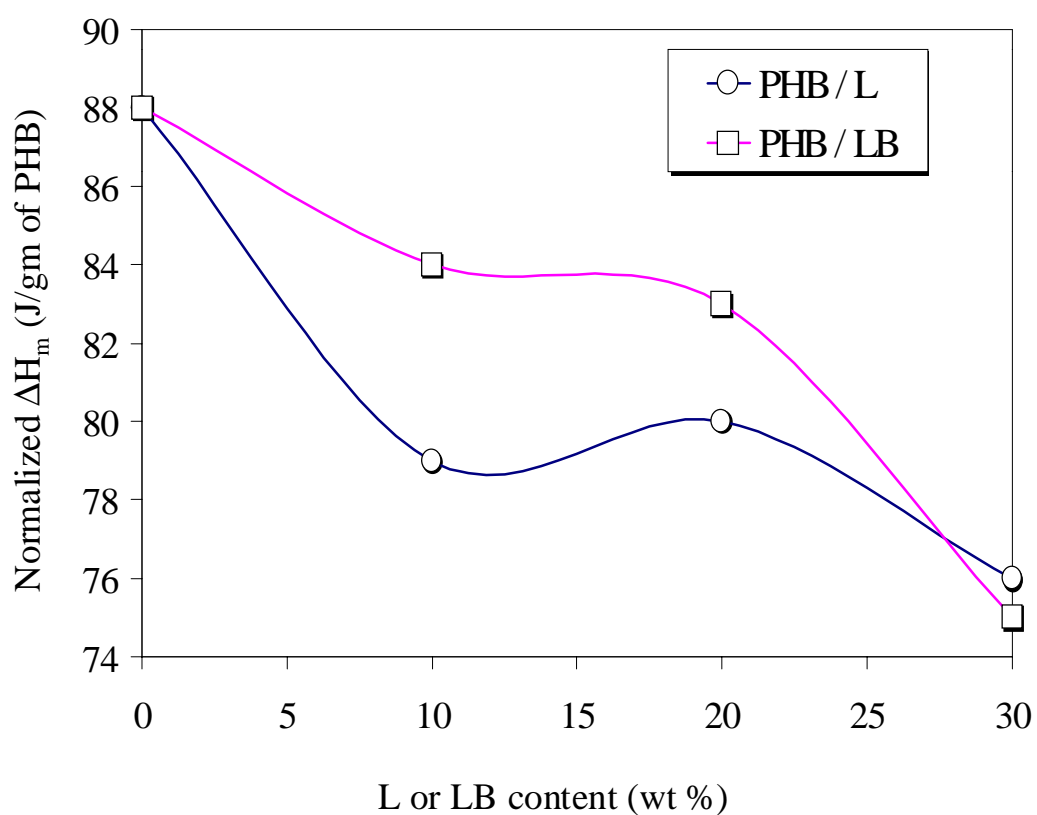


**Figure 4.6:** Normalized values of heat of fusion ( $\Delta H_m$ ) for PHB and L or LB blends.

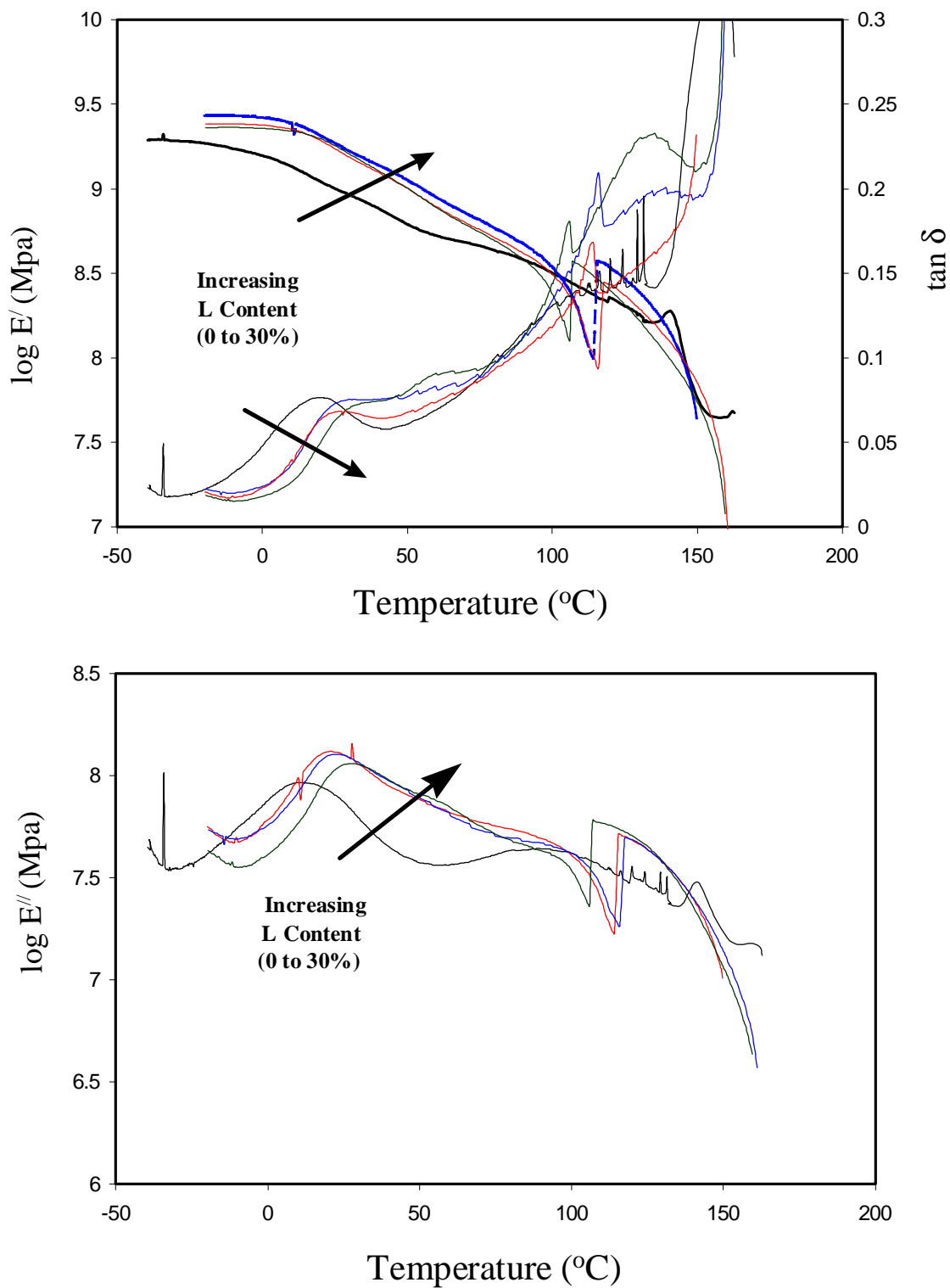


**Figure 4.7:** Temperature dependence of  $E'$ ,  $E''$  and  $\tan \delta$  of blends of PHB and L.

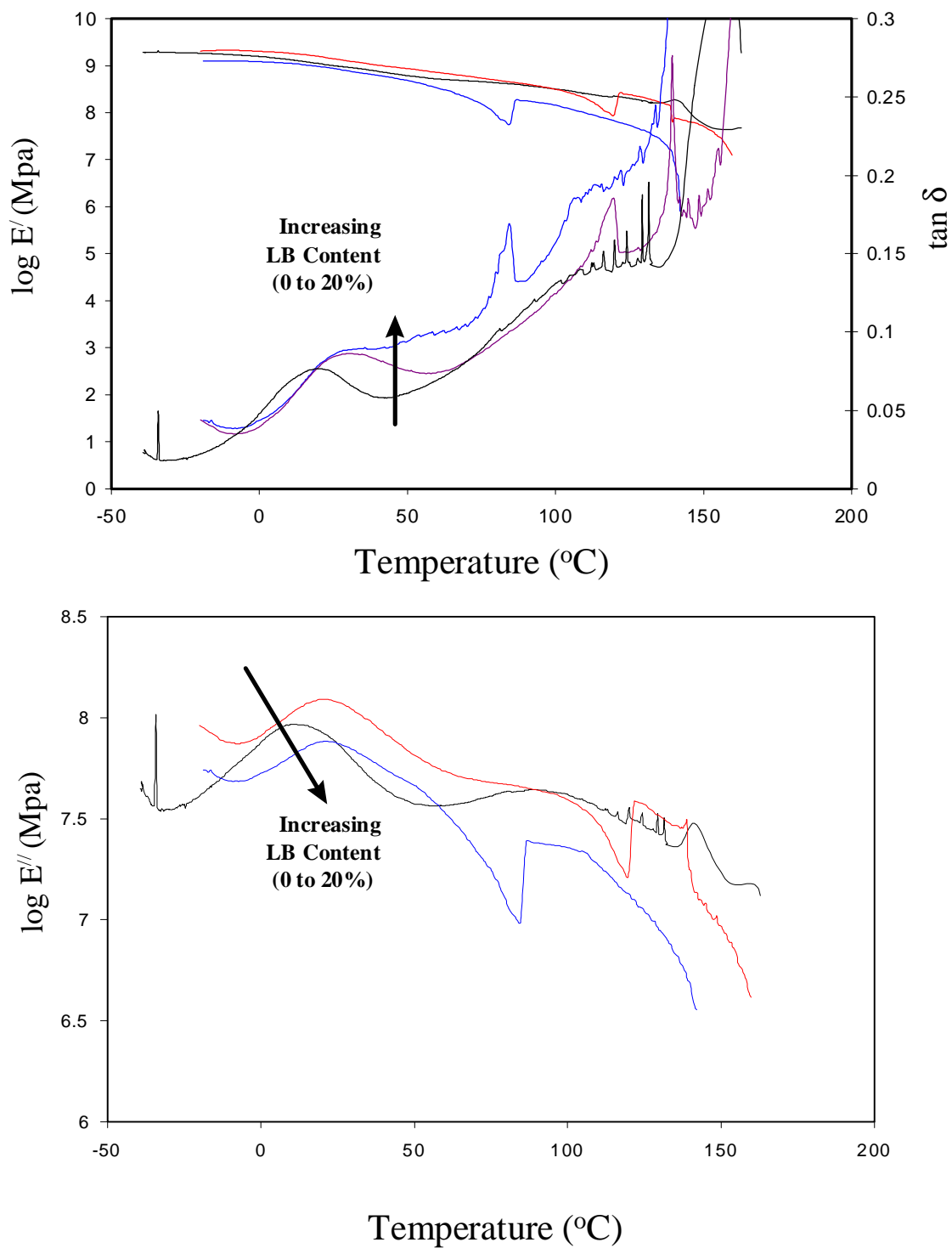


**Figure 4.8:** Temperature dependence of  $E'$ ,  $E''$  and  $\tan \delta$  of blends of PHB and LB.

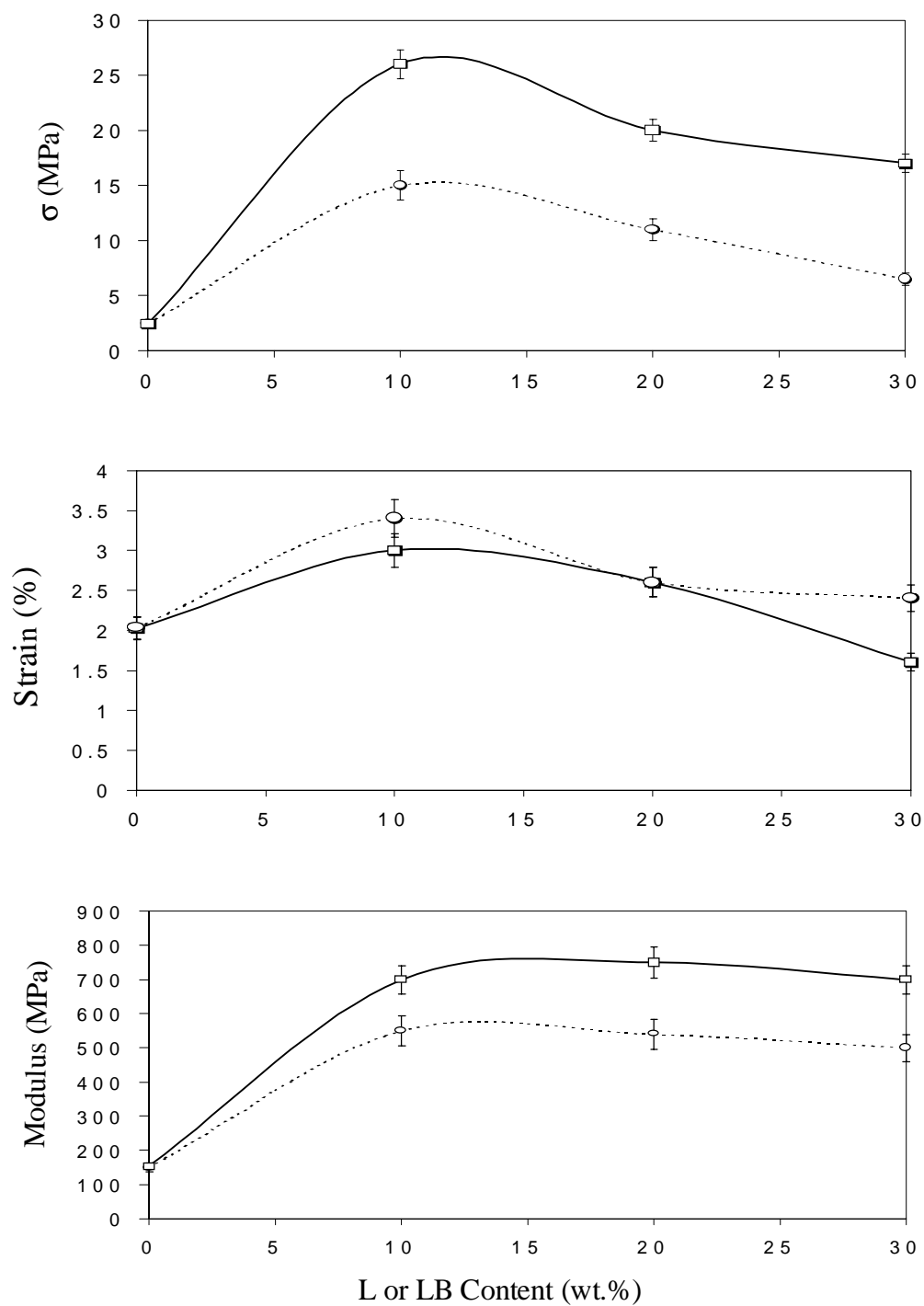


**Figure 4.9 :** (a) Tensile strength, (b) strain at break, and (c) modulus of blends of PHB and L or LB ( — L blends, - - - LB blends).

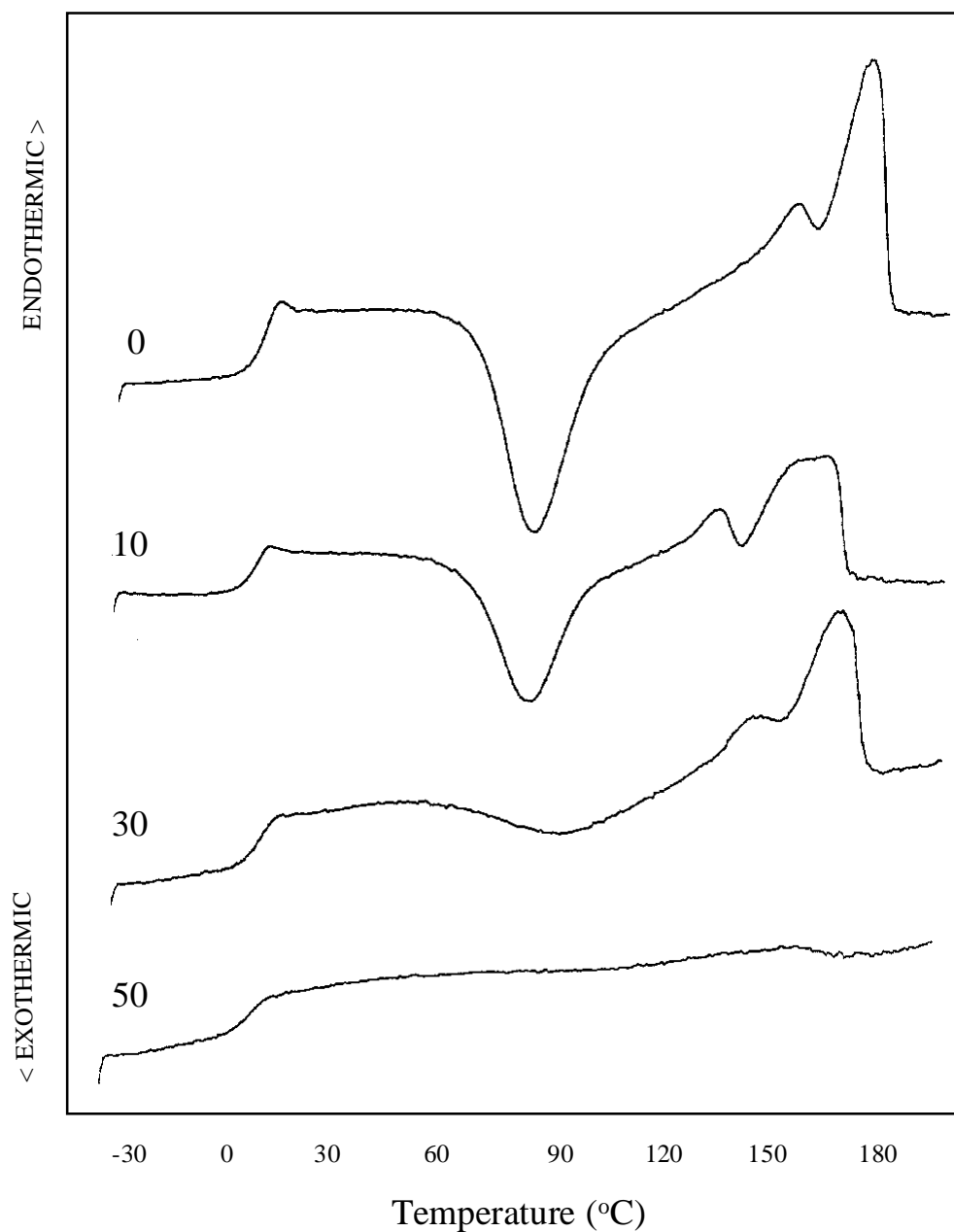


**Figure 4.10** : DSC thermograms of solvent ( $\text{CHCl}_3$ ) cast samples of PHBV and LB. Numbers on each curve denote LB content (wt.%) in the blend. These traces are from the second heating scan (after quenching from melt at a rate of  $300\text{ }^\circ\text{C/min}$ ).



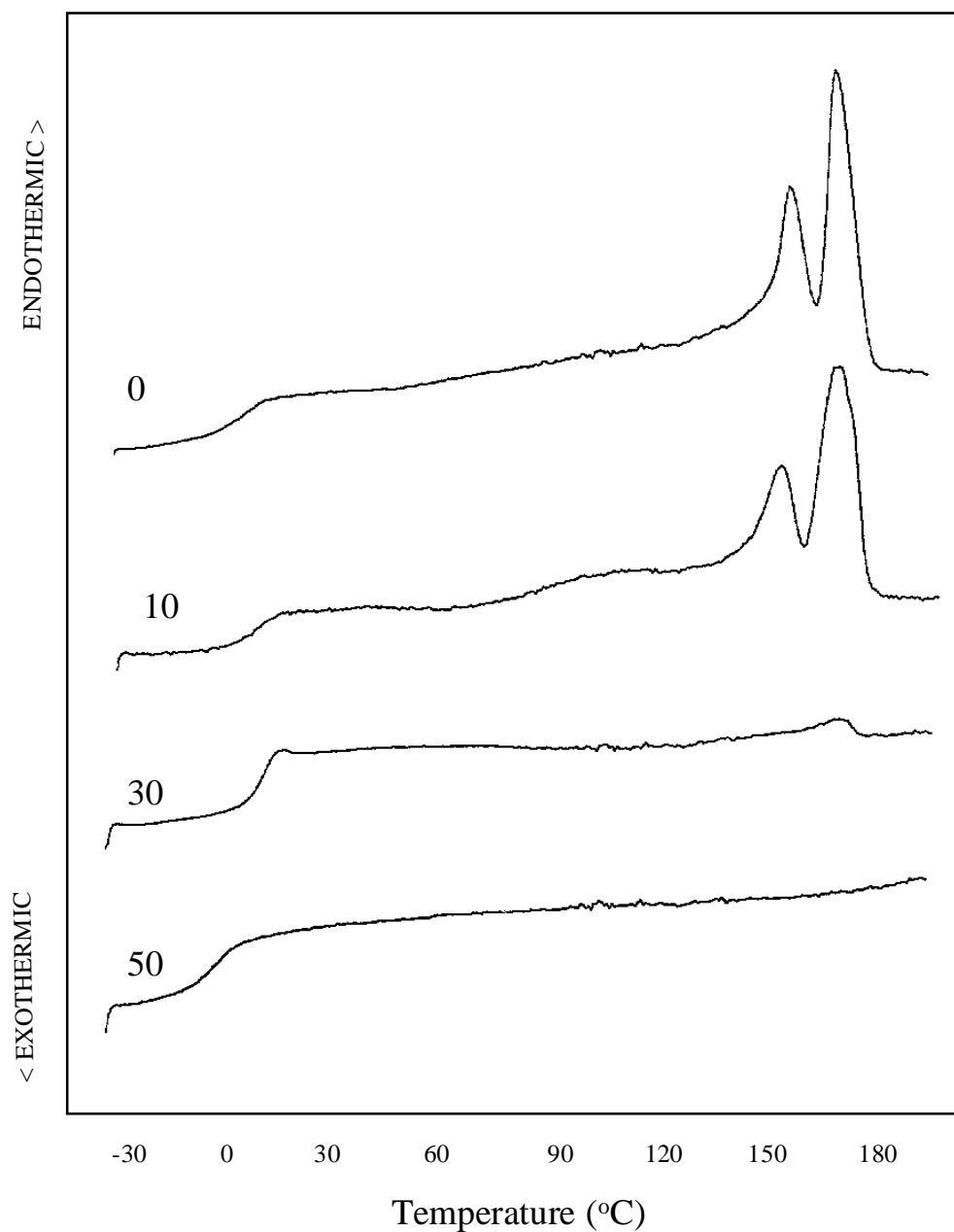


**Figure 4.11** : DSC thermograms of solvent ( $\text{CHCl}_3$ ) cast samples of PHBV and LB. Numbers on each curve denote LB content (wt.%) in the blend. These traces are from the second heating scan (after cooling from melt at a rate of  $10^\circ\text{C}/\text{min}$ ).

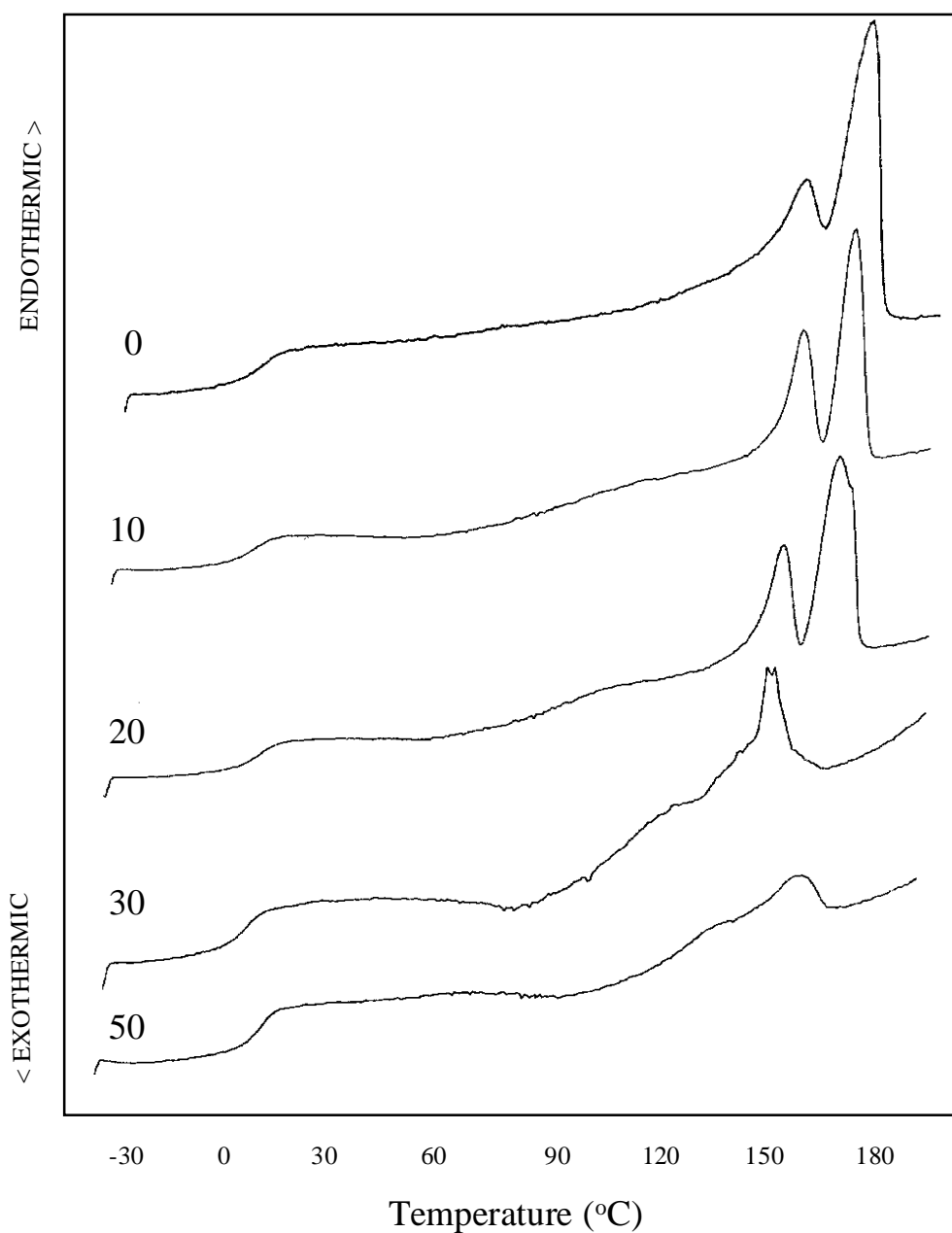


**Figure 4.12** : DSC thermograms of melt blended samples of PHBV and LB. Numbers on each curve denote LB content (wt.%) in the blend. These traces are from the second heating scan (after cooling from melt at a rate of 10 °C/min).

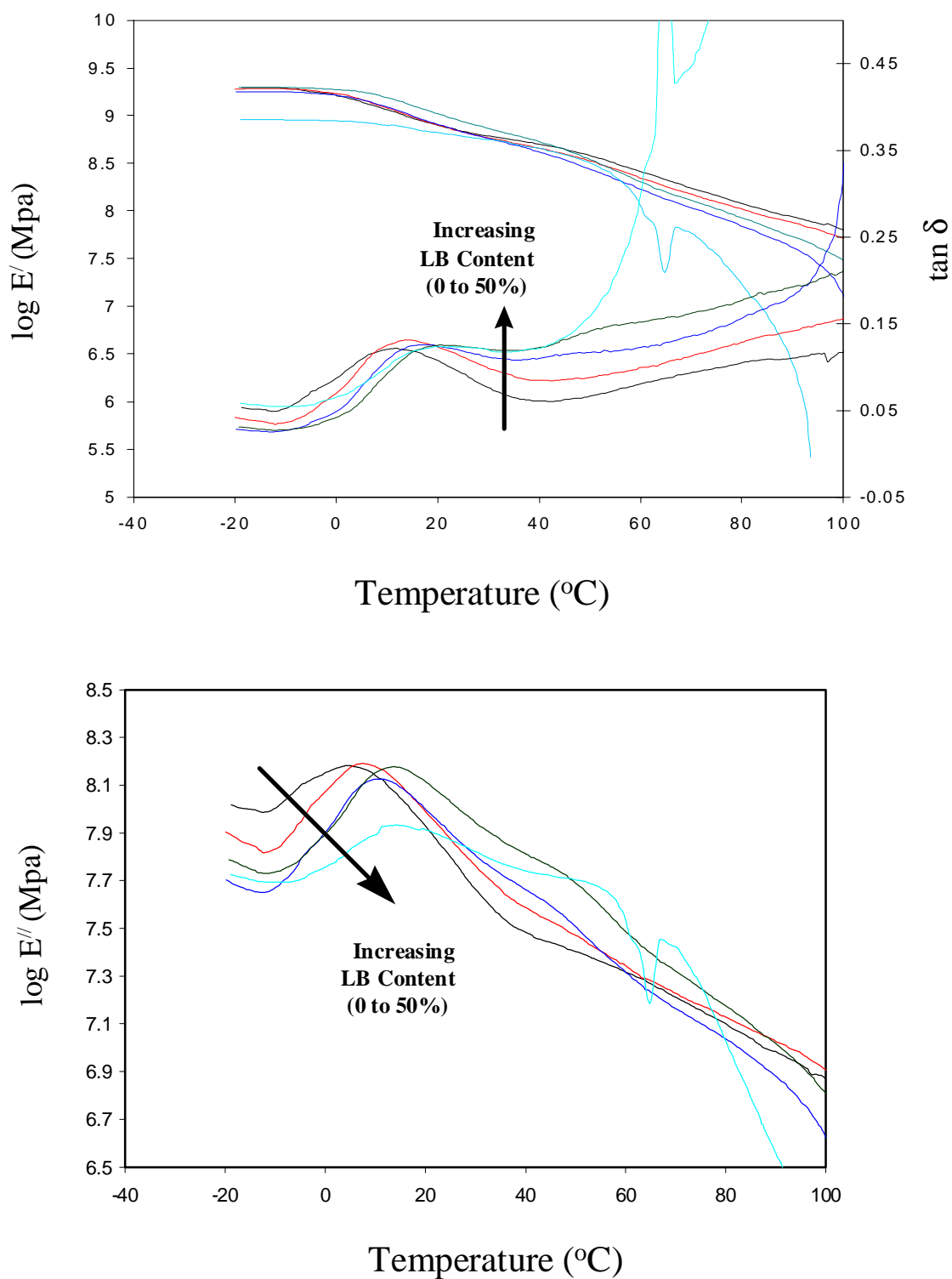


**Figure 4.13:** Temperature dependence of  $E'$ ,  $E''$  and  $\tan \delta$  of blends of PHBV and LB.

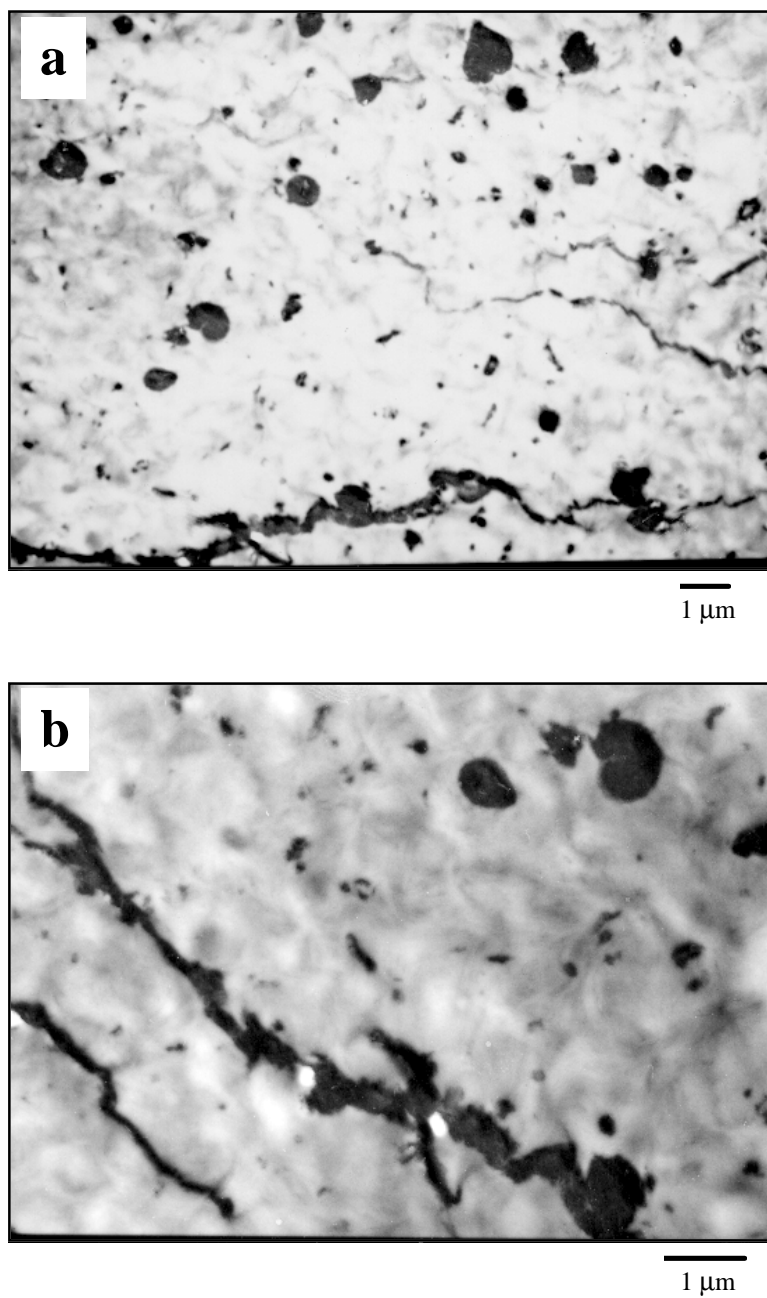


**Figure 4.14** : Transmission electron micrographs of solvent cast samples of PHBV / 20% LB blends with (a) magnification 4,800x and (b) magnification 10,000x.

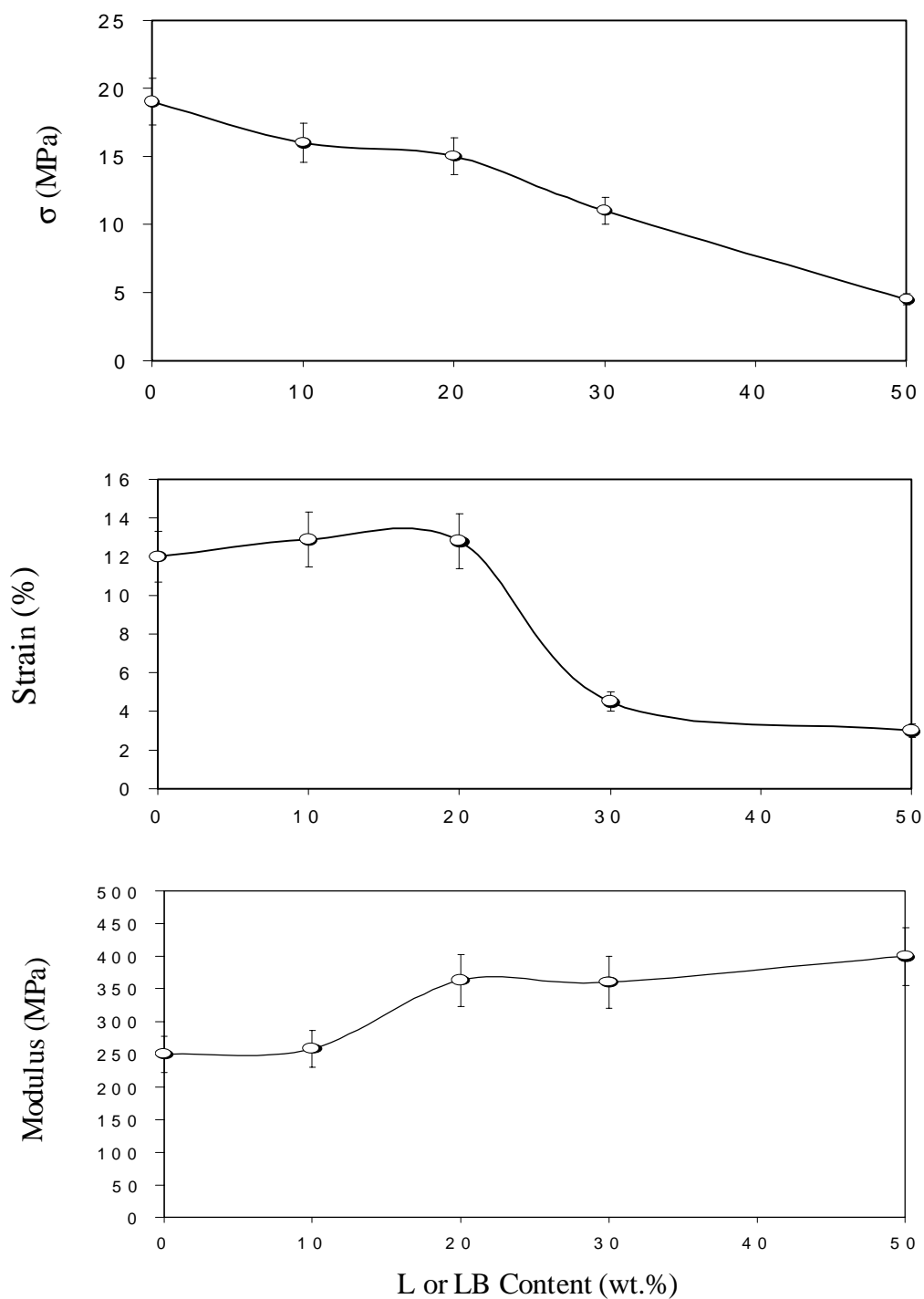


**Figure 4.15 :** (a) Tensile strength, (b) strain at break, and (c) modulus of blends of PHBV and LB.